LAWRENCE
LIVERMORE
NATIONAL
LABORATORY

LLNL-JRNL-866280

Response of fs-Laser Irradiated Diamond by Ultrafast Electron Diffraction

F. Bernal, E. J. Riffe, S. W. Devlin, S. Hamel, R. K. Lindsey, A. H. Reid, M. Mo, D. Luo, P. Kramer, X. Shen, A. Nadarajah, A. Stacey, S. Prawer, H. D. Whitley, C. P. Schwartz, R. J. Saykally

July 1, 2024

Journal of Physical Chemistry C

Disclaimer

Accepted for publication in the Journal of Physical Chemistry C

Response of fs-Laser Irradiated Diamond by Ultrafast Electron Diffraction

Franky Bernal[1,2], Erika J. Riffe[1], Shane W. Devlin[1,2,3], Sebastien Hamel[4], Rebecca K. Lindsey[4,5], Alexander H. Reid[6], Mianzhen Mo[6], Duan Luo[6,⊥], Patrick Kramer[6], Xiaozhe Shen[6], Athavan Nadarajah[7], Alastair Stacey[8,9], Steven Prawer[7], Heather D. Whitley[4], Craig P. Schwartz[3], Richard J. Saykally[1,2]**

[1]Department of Chemistry, University of California, Berkeley, Berkeley, CA 94720, USA

[2]Chemical Sciences Division, Lawrence Berkeley National Laboratory, Berkeley, CA 94720, USA

[3]Nevada Extreme Conditions Laboratory, University of Nevada, Las Vegas, Las Vegas, Nevada, 89154, USA

[4]Lawrence Livermore National Laboratory, 7000 East Ave, Livermore, CA 94550, USA

[5]Department of Chemical Engineering, University of Michigan, Ann Arbor, Michigan 48109, USA

[6]SLAC National Accelerator Laboratory, Menlo Park, CA 94025, USA

[⊥]Present address: Key Laboratory of Ultra-fast Photoelectric Diagnostics Technology, Xi'an Institute of Optics and Precision Mechanics, Chinese Academy of Sciences, Xi'an 710119, China.

[7]School of Physics, The University of Melbourne, Parkville, Victoria, 3010, Australia

[8]School of Science, RMIT University, Melbourne, Victoria, 3000, Australia

[9]Princeton Plasma Physics Laboratory, Princeton University, Princeton, New Jersey 08540, USA

Corresponding Authors

Craig P. Schwartz*

University of Nevada, Las Vegas, Las Vegas, Nevada 89154, USA.

craig.schwartz@unlv.edu

Richard J. Saykally*

Department of Chemistry, University of California, Berkeley, Berkeley, CA 94720, USA.

saykally@berkeley.edu

Abstract

Structural details of the proposed solid-liquid phase transition of carbon have remained elusive, despite years of study. While it is theorized that novel carbon materials form from a liquid precursor, experimental studies have lacked the temporal and spatial resolution necessary to fully characterize the purported liquid state. Here we utilize megaelectronvolt- ultrafast electron diffraction (MeV-UED) to study laser irradiated sub-micron diamond thin films in a pump-probe scheme with picosecond time resolution to visualize potential structural changes of excited diamond. We probe the structure of diamond using a combination of fluences (13, 40 J/cm^2) and time delays (10, 25, 100 ps), but observe negligible changes in the static diffraction pattern of diamond and an overall decrease in diffraction intensity up to 100 ps after the excitation pulse. We thus conclude that no appreciable amount of liquid or graphitized carbon is present and highlight the structural resilience of bulk diamond to intense 800 nm ultrafast laser pulses.

Introduction

Novel carbon materials are of much current interest, as their applications could engender profound advances in the areas of catalysis, energy storage, CO_2 conversion, and nuclear waste management[1–4]. Theoretical studies have suggested that the liquid phase of carbon may be the precursor to new exotic carbon nanostructures[5,6]. However, without reliable experimental evidence addressing the structure of liquid carbon, present day theoretical models remain limited in their ability to understand and predict the formation of novel forms of carbon. Given the planetary core-level pressures and temperatures required to successfully melt carbon without sublimation, characterizing its liquid state by table-top experiments has remained challenging[7]. Experimental evidence of melted carbon was first reported by Bundy in 1963, who performed flash-heating experiments on graphite rods inside a high-pressure cell[8]. Since then, a variety of methods have been used to melt carbon, including shock compression, electrical heating, and laser irradiation[8–11]. Numerous types of carbon targets have been examined (e.g. amorphous carbon (a-C), highly ordered pyrolytic graphite (HOPG), and diamond), with sample thicknesses ranging from angstroms to millimeters[8,11–13]. Under laboratory conditions, as carbon samples are non-thermally melted, the liquid phase is claimed to exist only briefly before rapidly evaporating. Melting carbon samples via irradiation with ultrafast optical pulses has become a common approach; however, the observation window of the liquid state is also limited by hydrodynamic expansion and ablation[14,15]. Therefore, attempts to characterize the liquid have typically relied on optical measurements that operate on short timescales. Various groups have employed X-ray spectroscopy and optical reflectivity experiments to characterize non-thermally melted carbon samples; however, these studies have often reached conflicting conclusions[12,14,16–

[18]. New tools with state-of-the-art time resolution and enhanced signal-to-noise ratios are clearly necessary to unambiguously characterize the structure of the transient liquid carbon state.

Given diamond's unique thermal and optical properties, there is great potential for its applications for optics and electronics[19]. Advances in chemical vapor deposition (CVD) instrumentation have increased the production of highly-ordered diamond samples[20]. Consequently, much effort has been directed towards examining the resilience of lab-grown diamonds, including their damage threshold from laser sources[21,22]. With sufficient energy, graphitization of diamond occurs whereby the diamond FCC lattice structure transforms into a graphite-like structure[23]. Reports of laser induced graphitization of diamond samples have established that a single laser pulse can generate a change in the diamond structure near the surface. For femtosecond laser pulses, the graphitization threshold has been reported to be ca. 0.3 - 4 J/cm^2 [24,25,23]. Fluences greater than 30 J/cm^2 have been used for the graphitization of bulk diamond samples[25]. While this phase transition in the carbon structure has been extensively studied as a method for generating HOPG, the mechanistic details have only recently been explored[26,23,27]. Excitation from an ultrafast laser pulse results in absorption of energy occurring on the order of femtoseconds, which drives the diamond into a nonequilibrium state well before the surrounding structure can respond[21]. Probing such an excited diamond in the picosecond time regime after the absorbed energy has begun to dissipate into the bulk lattice should provide insight into the structural evolution of the graphitization process, and evidence of whether a transient liquid carbon phase is involved.

In this work, we excite sub-micron samples of single crystal diamond films using ultrafast 800 nm laser pulses and probe the structure using single-shot megaelectronvolt-ultrafast electron diffraction (MeV-UED)[28]. Given the increased time resolution of modern MeV-UED, we are able to generate static diffraction images of diamond and provide time-dependent snapshots of the transient atomic structure several picoseconds after excitation[29]. Changes to the atomic structure (i.e. solid-liquid or solid-solid phase transitions) induced by the excitation pulse are evidenced in the diffraction pattern[30,31]. Mo et al. have successfully demonstrated the utility of this technique by monitoring the heterogeneous and homogeneous melting regimes of gold thin films. Their study revealed the formation of Debye-Scherrer rings between 100 - 1000 ps at low energy densities, and between 10 - 20 ps at higher energy densities. In the case of diamond melting, we would similarly expect the rigid molecular structure to evolve into a disordered liquid state and the corresponding diffraction pattern to exhibit Debye-Scherrer rings[30,32]. Tracking the evolution of structural changes with MeV-UED at various time delays could provide details underlying the development and validation of high-energy density physical models, and could thus greatly advance our understanding of the formation of unique carbon materials[33]. Our findings herein highlight the remarkable resilience of the bulk diamond structure, as it appears to remain unaltered for up to 100 ps after excitation from two different laser fluences, and indicates that a liquid state does not generally form following the excitation of diamond.

Experimental Methods

The fabrication process for producing ultra-thin Type IIa diamond membrane windows with an <100> orientation entailed a multi-step technique[34]. The key steps involved growing a high-

quality single-crystal diamond layer on a seed, fusing the overgrowth sample to a polycrystalline diamond scaffold, lifting off the overgrowth layer from the seed, and then precisely thinning the lifted-off layer to achieve the desired membrane thickness. The single-crystal membrane is only in physical contact with the polycrystalline scaffold, except near the edges of the sample where there is some chemical fusing[34]. Each window has a length and width of 170 μm and a maximum thickness of approximately 300 nm. Raman spectra of individual windows were used to check for non-diamond carbon phases. Photoluminescence spectra obtained at room temperature indicate that the membrane windows are free of defects, which suggests that common defects such as nitrogen vacancies (NVs) and silicon vacancies (SiVs) are present below minimum detection levels.

Ultrafast electron diffraction experiments were conducted at the MeV-UED facility at SLAC National Accelerator Laboratory and are depicted in Figure 1. A Ti:sapphire laser outputting 800 nm, ~75 fs pulses was used to excite individual windows at fluences of 13 J/cm^2 (200 μm FWHM diameter) and 40 J/cm^2 (100 μm FWHM diameter). The MeV-UED facility provided accelerated electron pulses (3.7 MeV, ~100 μm diameter) that were directed normal to the diamond windows in transmission geometry. Pump and probe pulses were synchronized and kept spatially overlapped as the target windows were raster-scanned. Samples were probed at 10, 25, and 100 ps time delays following excitation at two different pump fluences (13 and 40 J/cm^2). Static and post-excitation diffraction pattern pairs were recorded by a phosphor-based detector, binned according to fluence and time delay, then averaged (typically 4-5 windows per time delay). All diamond windows used in the analysis were unaffected by the probe pulse and confirmed to have been fully destroyed after the excitation pulse.

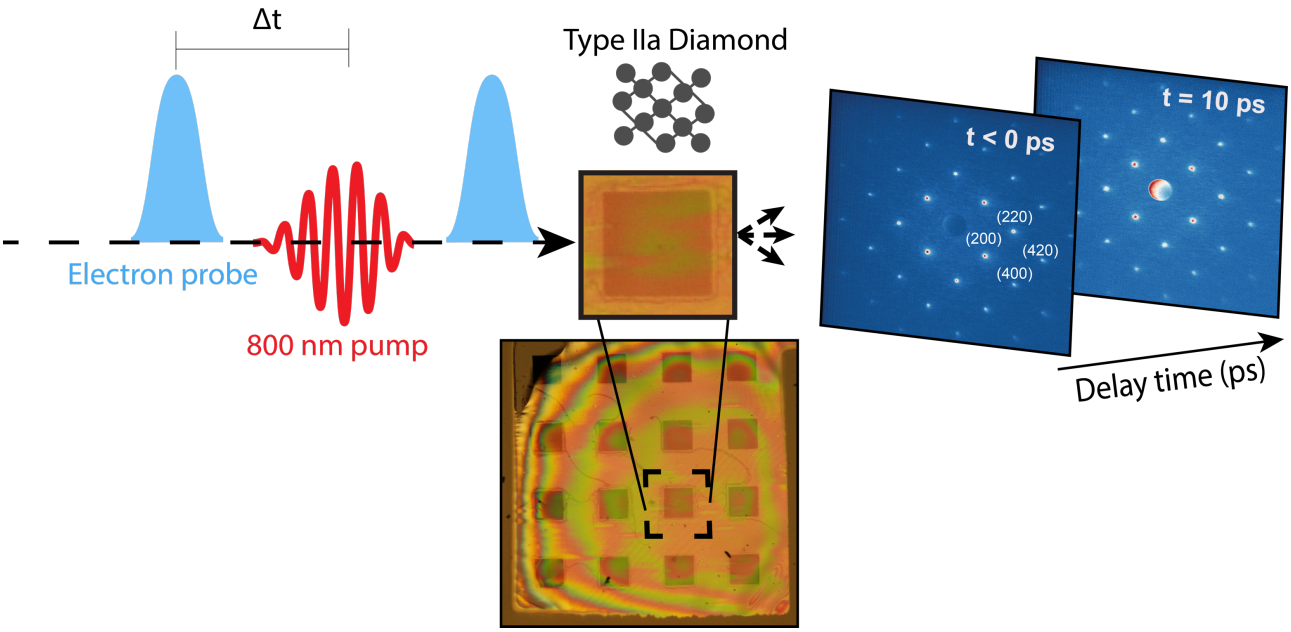

Figure 1. MeV-UED experimental setup. Individual diamond windows are probed with electron pulses before and after an 800 nm pump pulse (13 and 40 J/cm^2). The resulting diffraction images capture the initial sample structure and changes induced by the pump pulse. The diffraction images shown here were taken before (t < 0 ps) and after (t = 10 ps) excitation using a 13 J/cm^2 fluence.

Results and Discussion

On initial observation of the static diffraction patterns, there were no obvious qualitative changes pre- and post-pump for all time delays studied. Intensities of each time-dependent diffraction image were subtracted from initial static images to generate the diffraction patterns in Figure 2A-C at 10, 25, and 100 ps, respectively. From these differential diffraction images, the intensity of the diffraction peaks decreases after being exposed to the pump pulse (13 J/cm^2). Previous studies have attributed scattering intensity decreases in single crystalline materials to strongly driven electronic phase transitions occurring on the order of ca. 100 fs post-excitation[35].

Additionally, thermal effects leading to increased atomic vibrations are well-known to cause decreases in scattering intensity via the Debye-Waller factor[36]. Here, we observe no obvious streaking or positional shifts in the diffraction peaks after excitation, nor do we see any indication of Debye-Scherrer rings forming.

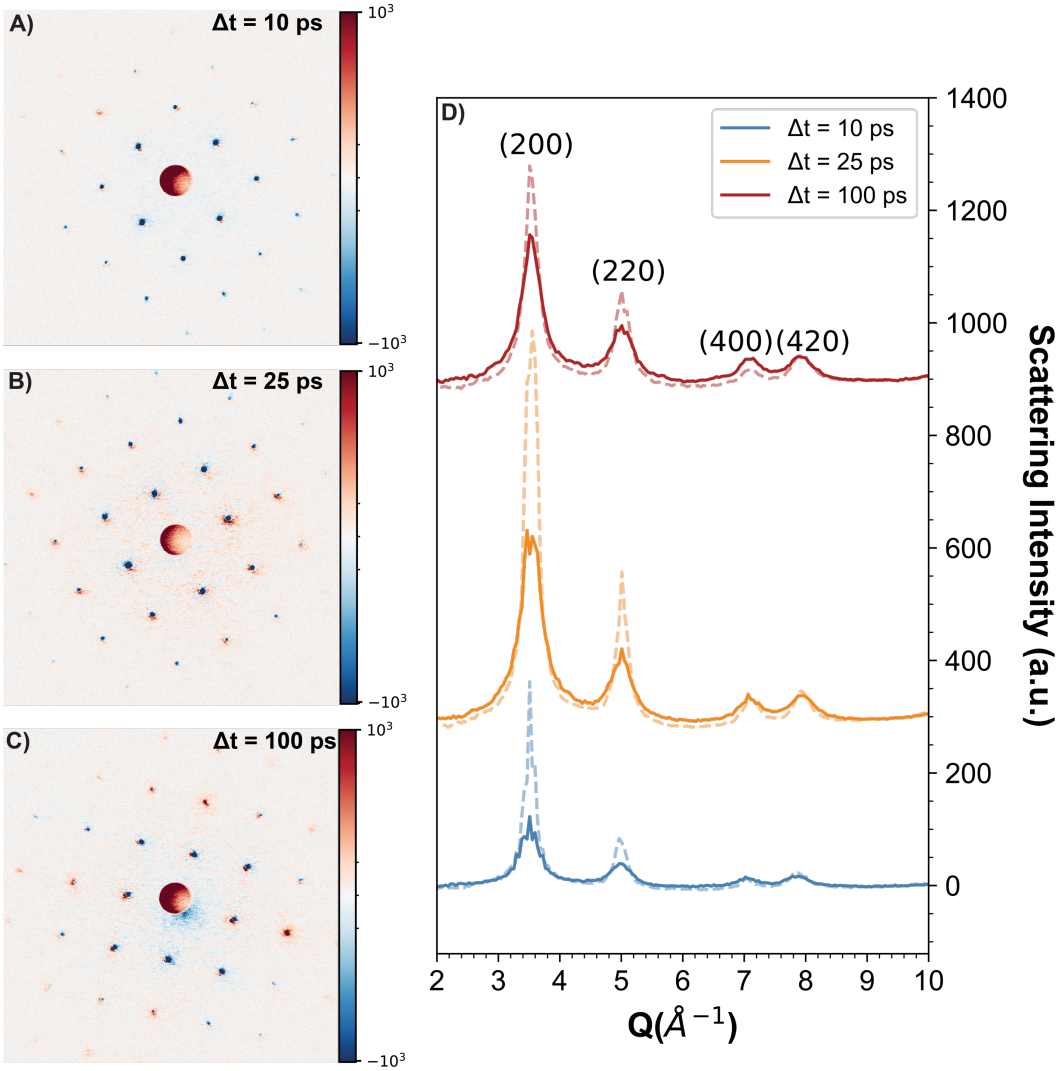

Figure 2. MeV-UED diffraction studies of diamond thin films before and after exposure to a non-thermal optical melting pulse (13 J/cm^2). (A to C) Differential diffraction patterns at three time delays: 10, 25, and 100 ps, respectively. Blue and red color shifts represent a decrease and increase in signal intensity, respectively, compared to the static diffraction pattern. (D) Radially

averaged patterns of diffraction data at each time delay. Dashed traces represent the initial signal at static conditions without the optical pump. The plots are offset from each other for clarity.

We radially averaged a collection of diffraction images at each time delay and converted to Q-space to generate the radial profile plots shown in Figure 2D. The dashed lines represent the pre-excitation patterns and the solid lines are post-excitation; each pre- and post-excitation pair is offset from the next for clarity. As seen in the differential diffraction images, each time delay displays the strongest decrease in intensity at the two low-Q peaks in Figure 2D, corresponding to the central peaks of the diffraction images ((200) and (220)). The two high-Q peaks exhibit little to no change in signal intensity post-excitation ((400) and (420)). The intensity decreases displayed here may be a result of strongly driven diamond undergoing initial bond breaking followed by further lattice effects (i.e. heating and ablation) at longer time delays. If the intensity decreases here were solely due to Debye-Waller effects, we would expect the local structures (high-Q peaks) to distort and diminish in intensity before the long-range structures (low-Q peaks)[30,35,37,38]. It is unclear why the high-Q peaks remain post-excitation at the various time delays studied here, but this may be an indication of other non-Debye-Waller effects occurring. Overall, the radial profile plots display a lack of significant broadening or shifting in the peaks after excitation.

In Figure 3, we used a 40 J/cm^2 fluence to excite diamond thin films and probed their structure at the same time delays used in Figure 2. As shown previously for gold thin films, increasing the pump fluence can affect melting dynamics and shorten the time needed for liquid state formation[30]. Therefore, studying diamond samples excited with a higher fluence allows access to structures at different pressure and temperature conditions. Again, we are not able to discern any

noticeable changes to the diffraction patterns at all time delays, as is indicated by the differential diffraction patterns and radial profile plots in Figure 3. Here, the 100 ps data reveals a drastic decrease in intensity noticeable even in the high-Q peaks and may be evidence of increased sample ablation or structural disordering due to the increased fluence. If the melting dynamics are indeed accelerated at an increased fluence, it is surprising that the 10 and 25 ps data at both 13 and 40 J/cm^2 fluences experience similar intensity decreases. This suggests that the bulk diamond structure is largely unaffected by the excitation pulses used here.

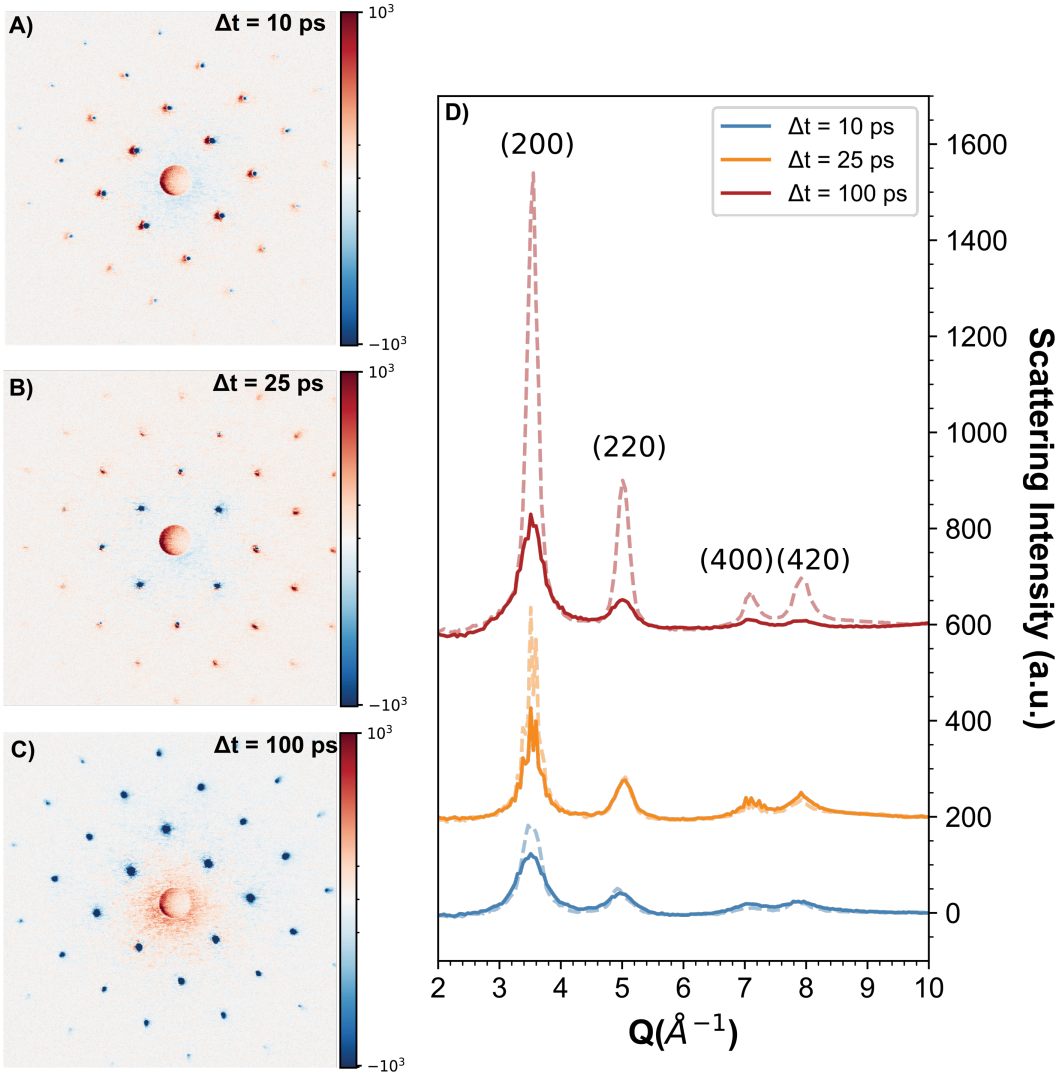

Figure 3. MeV-UED diffraction studies of diamond thin films before and after exposure to a non-thermal optical melting pulse (40 J/cm^2). (A to C) Differential diffraction patterns at three time delays: 10, 25, and 100 ps, respectively. Blue and red color shifts represent a decrease and increase in signal intensity, respectively, compared to the static diffraction pattern. (D) Radially averaged patterns of diffraction data at each time delay. Dashed traces represent the initial signal at static conditions without the optical pump. The plots are offset from each other for clarity.

For comparison, we simulated radially averaged diffraction patterns using molecular dynamics (MD) simulations where the forces governing the dynamics were either calculated from the electronic structure using Density Functional Theory (DFT) or calculated using the ChIMES interatomic potential. Figure 4A shows the computed radial distribution function and scattering intensity from a DFT-MD calculation of carbon at 5000K and 2.27 g/cm^3 performed using the VASP software as well as results from our previously reported simulations at 2.1g/cm^3 using the ChIMES-MD method as implemented in the LAMMPS simulation code at temperatures of 7000, 14000, and 17000 K[39–41]. The DFT simulation was carried out using the VASP code using the Perdew-Burke-Ernzerhof (PBE) functional[42–47]. The simulated radial distribution function is in good agreement with a previous study[18]. A Fourier transform of the simulated radial distribution functions from VASP and LAMMPS was done to convert to reciprocal space (Figure 4B). If the diamond was undergoing a solid-liquid phase transition, we would expect the single-crystal peaks to disappear in the profile plots and the emergence of a broad liquid peak near 5.5 Å^{-1}, as indicated by the simulated structure factor trace in Figure 4B. From the simulations in Figure 4 we observe increasing temperature suppresses the intensity of the peaks in the computed radial

distribution functions and broadens the corresponding structure factor, a trend not seen in the experimental data.

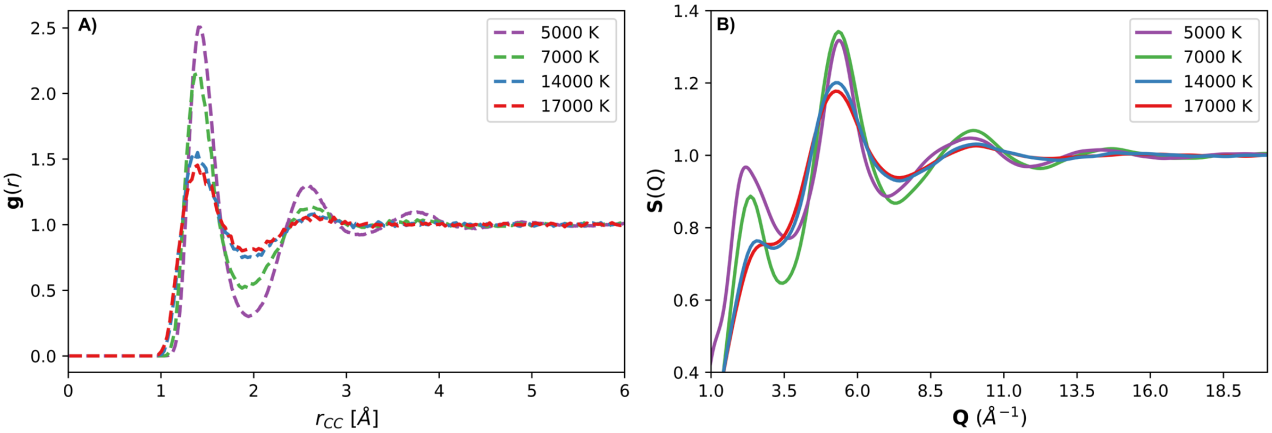

Figure 4. Carbon simulations using DFT-MD (5000K and 2.27 g/cm^3) and ChIMES-MD (7000, 14000, and 17000 K and 2.1 g/cm^3). (A) Simulated radial distribution functions of carbon. (B) Simulated structure factor of carbon. The small modulations < 3.5 Å^{-1} are artifacts of the Fourier transform and the finite size of the simulation.

These results are surprising, given previous reports of liquid carbon formation and diamond graphitization[12,23]. Both processes involve a transformation of the initial diamond structure, yet our data do not capture any significant differences between pre- and post-excited samples. Studies suggest that liquid carbon formation occurs within the first few picoseconds for laser excited amorphous carbon[18]. Therefore, a 10 ps time delay between the pump and probe would have provided enough time for any liquid carbon formed to equilibrate and begin to cool or evaporate. Longer time delays, 25 and 100 ps, may have provided insight into the lifetime of liquid carbon or the formation of new structures. However, it appears that our diamond samples are not melted using the fluences recorded here; to suggest that bulk diamond was melted by the

excitation pulse and then cooled to its original structure within the first 10 ps is unphysical. We see no evidence for a bulk melted structure and any small volumes of surface generated liquid would have been displaced due to surface expansion and evaporation. In addition to the lack of observed melting, we surprisingly do not see structural indications of diamond graphitization.

We are aware of only a few studies addressing the successful melting of a diamond-like sample but that is not the case for diamond graphitization, which is well studied[17]. The pump pulses used here are well above the threshold for graphitization, although there is debate regarding the rate of graphitized diamond production per pulse. A single 100 fs, 10 J/cm^2 laser pulse has been demonstrated to cause graphitization in < 20 nm of diamond[48] and with fluences as high as 200 J/cm^2 reach a max ablation rate of about 100 nm per pulse. Clearly, the pulse energies needed to increase graphitization thickness do not scale linearly and are wavelength dependent[24]. This may account for the diamond scattering patterns in Figure 2 and Figure 3 exhibiting striking similarities despite the increase in fluence, as graphitization may not have extended as deeply into the bulk. However, based on previous single-shot graphitization data, approximately 80 nm of graphitized diamond should have been produced from our single-shot excitation pulses[23].

Since no substantial changes to the initial diffraction pattern of the diamond are observed after excitation with a 13 or 40 J/cm^2 fluences, this suggests that the samples are directly sublimating and not evolving through a phase transition. If a sizeable volume of diamond sample was graphitized by a single pulse, then we would expect to see traces of a hexagonal diffraction pattern in the differential diffraction images. Decreases in diamond scattering intensity have been previously attributed to reorganization of the crystal structure in addition to Debye-Waller

effects, which could be an indication of trace amounts of graphitization occurring here[49], but the diffraction pattern remains consistent with that of diamond, and no signs of new peaks emerging due to graphite are found. It is unlikely that the higher fluence generates more graphite than the lower fluence here, since the observed decrease in diffraction intensity remains similar for both at early time delays. It is more likely that the diamond samples are ablated by the pump pulse, which would result in the diamond directly sublimating, thereby reducing the sample thickness and causing localized heating, two processes that would reduce the scattering intensity. This explanation would also agree with laser machined images of polycrystalline diamond samples, wherein femtosecond pulses formed a minimal graphitized layer compared to nanosecond pulses[50]. At long time delays, viz. 1 ms, no scattering intensity is detected, as samples damaged by the pump pulse catastrophically shattered likely due to their free-standing nature.

Our results thus seem to conflict with the interpretation of previous studies wherein researchers observed indication of liquid carbon formation from diamond-like samples[16,17]. It is possible that these studies, which are more sensitive to interfacial effects given their different experimental approaches, may have evidenced the effects of a plasma state or evaporation cloud formation which we do not see in the present experiment[12,51]. Since MeV-UED is not an interface specific technique, our work indicates that the majority of our diamond samples do not undergo a solid-liquid phase transition or graphitization for the fluences and wavelengths used here. Recent studies report the formation of liquid carbon at sub-picosecond time scales via XAS for a-C samples[18]. However, the inference of the liquid state from the XAS data is indirect, and the observed spectral changes could also be consistent with rearrangements of the carbon atoms due to vibrational motion rather than melting. Our recent work investigated the electronic structure of

diamond using time-resolved resonant inelastic x-ray scattering and observed no substantial changes following excitation that were indicative of a liquid state[52]. Similarly, our diffraction data presented here shows potential signs of slight disordering in the crystal structure, but we do not see a clear indicator of liquid formation. Still, we are not able to definitively rule out interfacial liquid carbon formation since it may be that our samples were too thick to accurately resolve surface confined liquid. Although 800 nm light is commonly used in literature to study a wide array of carbon materials, the photon energy supplied may not be sufficient to drive a significant portion of bulk diamond and the use of higher frequency light sources should be explored[53]. Future experiments with thinner diamond samples, sub-picosecond time-resolution, and higher photon energies are clearly required to disambiguate liquid carbon formation from other forms of carbon.

Conclusions

In summary, we used an ultrafast optical pump to non-thermally excite diamond thin films and probed the atomic structure as a function of time delay using state-of-the-art MeV-UED. Diamond samples were excited with laser fluences of 13 and 40 J/cm^2 at 10, 25 and 100 ps time delays. We observe a reduction in the intensity of the diamond diffraction pattern between 10 and 100 ps with no streaking or shifts in the peak positions. That these results are inconsistent with previous reports of liquid carbon formation and diamond graphitization but agree with our recent x-ray studies of nanocrystalline diamond suggests that continued efforts in characterizing the liquid state of carbon are necessary[52]. Unlike previous measurements, MeV-UED acts as a direct probe of the atomic structure and adds to the existing body of work on liquid carbon. We

determine with high certainty that no significant amount of our diamond sample structure transforms into a liquid state or undergoes graphitization. In a previous study, we investigated the electronic response of diamond and captured no obvious changes to the electronic structure following ultrafast laser excitation. Here, we complement that work and highlight that the bulk atomic structure of our diamond samples remains unchanged following excitation from intense near-IR femtosecond laser radiation.

Notes

The authors declare no competing financial interests.

Acknowledgements

FB and RJS were supported by the Department of Energy, Office of Basic Energy Sciences, through the Chemical Sciences Division at the Lawrence Berkeley National Laboratory under contract #CH403503. E.J.R. acknowledges support from CALSOLV/RESOLV-Bochum and the UC Office of the President within the Multicampus Research Programs and Initiatives. MeV-UED is operated as part of the Linac Coherent Light Source at the SLAC National Accelerator Laboratory, supported by the U.S. Department of Energy, Office of Science, Office of Basic Energy Sciences under Contract No. DE-AC02-76SF00515. This work was performed under the auspices of the U.S. Department of Energy by Lawrence Livermore National Laboratory under Contract DE-AC52-07NA27344. CPS and SWD received support from the U.S. Department of Energy, Office of Science, Office of Basic Energy Sciences initiative for clean energy manufacturing under Contract No. DE-SC0023355. Sample fabrication for this work was funded under the Australian Research Council (ARC) Linkage project (LP190100528) with industry partner the Israeli Center of Advanced Diamond Technologies.

References

(1) Lee, J.; Kim, J.; Hyeon, T. Recent Progress in the Synthesis of Porous Carbon Materials. *Advanced Materials* **2006**, *18* (16), 2073–2094. https://doi.org/10.1002/adma.200501576.

(2) Dai, L.; Karakas, O.; Cheng, Y.; Cobb, K.; Chen, P.; Ruan, R. A Review on Carbon Materials Production from Plastic Wastes. *Chemical Engineering Journal* **2023**, *453*, 139725. https://doi.org/10.1016/j.cej.2022.139725.

(3) Duan, X.; Xu, J.; Wei, Z.; Ma, J.; Guo, S.; Wang, S.; Liu, H.; Dou, S. Metal-Free Carbon Materials for CO2 Electrochemical Reduction. *Advanced Materials* **2017**, *29* (41), 1701784. https://doi.org/10.1002/adma.201701784.

(4) Belloni, F.; Kütahyali, C.; Rondinella, V. V.; Carbol, P.; Wiss, T.; Mangione, A. Can Carbon Nanotubes Play a Role in the Field of Nuclear Waste Management? *Environ. Sci. Technol.* **2009**, *43* (5), 1250–1255. https://doi.org/10.1021/es802764g.

(5) Narayan, J.; Bhaumik, A. Novel Phase of Carbon, Ferromagnetism, and Conversion into Diamond. *Journal of Applied Physics* **2015**, *118* (21), 215303. https://doi.org/10.1063/1.4936595.

(6) Galli, G.; Martin, R. M.; Car, R.; Parrinello, M. Ab Initio Calculation of Properties of Carbon in the Amorphous and Liquid States. *Phys. Rev. B* **1990**, *42* (12), 7470–7482. https://doi.org/10.1103/PhysRevB.42.7470.

(7) Bundy, F. P. Pressure-Temperature Phase Diagram of Elemental Carbon. *Physica A: Statistical Mechanics and its Applications* **1989**, *156* (1), 169–178. https://doi.org/10.1016/0378-4371(89)90115-5.

(8) Bundy, F. P. Melting of Graphite at Very High Pressure. *The Journal of Chemical Physics* **1963**, *38* (3), 618–630. https://doi.org/10.1063/1.1733715.

(9) Savvatimskiy, A. I. Measurements of the Melting Point of Graphite and the Properties of Liquid Carbon (a Review for 1963–2003). *Carbon* **2005**, *43* (6), 1115–1142. https://doi.org/10.1016/j.carbon.2004.12.027.

(10) Eggert, J. H.; Hicks, D. G.; Celliers, P. M.; Bradley, D. K.; McWilliams, R. S.; Jeanloz, R.; Miller, J. E.; Boehly, T. R.; Collins, G. W. Melting Temperature of Diamond at Ultrahigh Pressure. *Nature Phys* **2010**, *6* (1), 40–43. https://doi.org/10.1038/nphys1438.

(11) Brygoo, S.; Henry, E.; Loubeyre, P.; Eggert, J.; Koenig, M.; Loupias, B.; Benuzzi-Mounaix, A.; Rabec Le Gloahec, M. Laser-Shock Compression of Diamond and Evidence of a Negative-Slope Melting Curve. *Nature Mater* **2007**, *6* (4), 274–277. https://doi.org/10.1038/nmat1863.

(12) Hull, C. J.; Raj, S. L.; Saykally, R. J. The Liquid State of Carbon. *Chemical Physics Letters* **2020**, *749*, 137341. https://doi.org/10.1016/j.cplett.2020.137341.

(13) Kraus, D.; Vorberger, J.; Gericke, D. O.; Bagnoud, V.; Blažević, A.; Cayzac, W.; Frank, A.; Gregori, G.; Ortner, A.; Otten, A.; et al. Probing the Complex Ion Structure in Liquid Carbon at 100 GPa. *Phys. Rev. Lett.* **2013**, *111* (25), 255501. https://doi.org/10.1103/PhysRevLett.111.255501.

(14) Mincigrucci, R.; Principi, E.; Bencivenga, F.; Foglia, L.; Gessini, A.; Kurdi, G.; Simoncig, A.; Masciovecchio, C. Transient EUV Reflectivity Measurements of Carbon upon Ultrafast Laser Heating. *Photonics* **2017**, *4* (2), 23. https://doi.org/10.3390/photonics4020023.

(15) Perez, D.; Lewis, L. J. Ablation of Solids under Femtosecond Laser Pulses. *Phys. Rev. Lett.* **2002**, *89* (25), 255504. https://doi.org/10.1103/PhysRevLett.89.255504.

(16) Reitze, D. H.; Ahn, H.; Downer, M. C. Optical Properties of Liquid Carbon Measured by Femtosecond Spectroscopy. *Phys. Rev. B* **1992**, *45* (6), 2677–2693. https://doi.org/10.1103/PhysRevB.45.2677.
(17) Johnson, S. L.; Heimann, P. A.; MacPhee, A. G.; Lindenberg, A. M.; Monteiro, O. R.; Chang, Z.; Lee, R. W.; Falcone, R. W. Bonding in Liquid Carbon Studied by Time-Resolved X-Ray Absorption Spectroscopy. *Phys. Rev. Lett.* **2005**, *94* (5), 057407. https://doi.org/10.1103/PhysRevLett.94.057407.
(18) Principi, E.; Krylow, S.; Garcia, M. E.; Simoncig, A.; Foglia, L.; Mincigrucci, R.; Kurdi, G.; Gessini, A.; Bencivenga, F.; Giglia, A.; et al. Atomic and Electronic Structure of Solid-Density Liquid Carbon. *Phys. Rev. Lett.* **2020**, *125* (15), 155703. https://doi.org/10.1103/PhysRevLett.125.155703.
(19) Zhang, C.; Vispute, R. D.; Fu, K.; Ni, C. A Review of Thermal Properties of CVD Diamond Films. *J Mater Sci* **2023**, *58* (8), 3485–3507. https://doi.org/10.1007/s10853-023-08232-w.
(20) Lee, S.-T.; Lin, Z.; Jiang, X. CVD Diamond Films: Nucleation and Growth. *Materials Science and Engineering: R: Reports* **1999**, *25* (4), 123–154. https://doi.org/10.1016/S0927-796X(99)00003-0.
(21) Ali, B.; Litvinyuk, I. V.; Rybachuk, M. Femtosecond Laser Micromachining of Diamond: Current Research Status, Applications and Challenges. *Carbon* **2021**, *179*, 209–226. https://doi.org/10.1016/j.carbon.2021.04.025.
(22) Hsu, E. M.; Mailman, N. A.; Botton, G. A.; Haugen, H. K. Microscopic Investigation of Single-Crystal Diamond Following Ultrafast Laser Irradiation. *Appl. Phys. A* **2011**, *103* (1), 185–192. https://doi.org/10.1007/s00339-010-5986-4.
(23) Kononenko, V. V. Modification of Diamond Surface by Femtosecond Laser Pulses. *Photonics* **2023**, *10* (10), 1077. https://doi.org/10.3390/photonics10101077.
(24) Preuss, S.; Stuke, M. Subpicosecond Ultraviolet Laser Ablation of Diamond: Nonlinear Properties at 248 Nm and Time-resolved Characterization of Ablation Dynamics. *Applied Physics Letters* **1995**, *67* (3), 338–340. https://doi.org/10.1063/1.115437.
(25) Kononenko, V. V.; Khomich, A. A.; Khomich, A. V.; Khmelnitskii, R. A.; Gololobov, V. M.; Komlenok, M. S.; Orekhov, A. S.; Orekhov, A. S.; Konov, V. I. Highly Oriented Graphite Produced by Femtosecond Laser on Diamond. *Applied Physics Letters* **2019**, *114* (25), 251903. https://doi.org/10.1063/1.5097986.
(26) Evans, T.; James, P. F.; Ditchburn, R. W. A Study of the Transformation of Diamond to Graphite. *Proceedings of the Royal Society of London. Series A. Mathematical and Physical Sciences* **1997**, *277* (1369), 260–269. https://doi.org/10.1098/rspa.1964.0020.
(27) Li, B.; Liu, B.; Luo, K.; Tong, K.; Zhao, Z.; Tian, Y. Discovery of Gradia between Graphite and Diamond. *Acc. Mater. Res.* **2024**, *5* (5), 614–624. https://doi.org/10.1021/accountsmr.4c00029.
(28) Mo, M. Z.; Shen, X.; Chen, Z.; Li, R. K.; Dunning, M.; Sokolowski-Tinten, K.; Zheng, Q.; Weathersby, S. P.; Reid, A. H.; Coffee, R.; et al. Single-Shot Mega-Electronvolt Ultrafast Electron Diffraction for Structure Dynamic Studies of Warm Dense Matter. *Review of Scientific Instruments* **2016**, *87* (11), 11D810. https://doi.org/10.1063/1.4960070.
(29) Filippetto, D.; Musumeci, P.; Li, R. K.; Siwick, B. J.; Otto, M. R.; Centurion, M.; Nunes, J. P. F. Ultrafast Electron Diffraction: Visualizing Dynamic States of Matter. *Rev. Mod. Phys.* **2022**, *94* (4), 045004. https://doi.org/10.1103/RevModPhys.94.045004.

(30) Mo, M. Z.; Chen, Z.; Li, R. K.; Dunning, M.; Witte, B. B. L.; Baldwin, J. K.; Fletcher, L. B.; Kim, J. B.; Ng, A.; Redmer, R.; et al. Heterogeneous to Homogeneous Melting Transition Visualized with Ultrafast Electron Diffraction. *Science* **2018**, *360* (6396), 1451–1455. https://doi.org/10.1126/science.aar2058.

(31) Siwick, B. J.; Dwyer, J. R.; Jordan, R. E.; Miller, R. J. D. An Atomic-Level View of Melting Using Femtosecond Electron Diffraction. *Science* **2003**, *302* (5649), 1382–1385. https://doi.org/10.1126/science.1090052.

(32) Takagi, M. Electron-Diffraction Study of Liquid-Solid Transition of Thin Metal Films. *J. Phys. Soc. Jpn.* **1954**, *9* (3), 359–363. https://doi.org/10.1143/JPSJ.9.359.

(33) Scott, H. A.; Hansen, S. B. Advances in NLTE Modeling for Integrated Simulations. *High Energy Density Physics* **2010**, *6* (1), 39–47. https://doi.org/10.1016/j.hedp.2009.07.003.

(34) Habib Piracha, A.; Ganesan, K.; M. Lau, D. W.; Stacey, A.; P. McGuinness, L.; Tomljenovic-Hanic, S.; Prawer, S. Scalable Fabrication of High-Quality, Ultra-Thin Single Crystal Diamond Membrane Windows. *Nanoscale* **2016**, *8* (12), 6860–6865. https://doi.org/10.1039/C5NR08348F.

(35) Harb, M.; Ernstorfer, R.; Hebeisen, C. T.; Sciaini, G.; Peng, W.; Dartigalongue, T.; Eriksson, M. A.; Lagally, M. G.; Kruglik, S. G.; Miller, R. J. D. Electronically Driven Structure Changes of Si Captured by Femtosecond Electron Diffraction. *Phys. Rev. Lett.* **2008**, *100* (15), 155504. https://doi.org/10.1103/PhysRevLett.100.155504.

(36) Vila, F. D.; Rehr, J. J.; Rossner, H. H.; Krappe, H. J. Theoretical X-Ray Absorption Debye-Waller Factors. *Phys. Rev. B* **2007**, *76* (1), 014301. https://doi.org/10.1103/PhysRevB.76.014301.

(37) Siwick, B. J.; Dwyer, J. R.; Jordan, R. E.; Miller, R. J. D. Femtosecond Electron Diffraction Studies of Strongly Driven Structural Phase Transitions. *Chemical Physics* **2004**, *299* (2), 285–305. https://doi.org/10.1016/j.chemphys.2003.11.040.

(38) Wu, J.; Tang, M.; Zhao, L.; Zhu, P.; Jiang, T.; Zou, X.; Hong, L.; Luo, S.-N.; Xiang, D.; Zhang, J. Ultrafast Atomic View of Laser-Induced Melting and Breathing Motion of Metallic Liquid Clusters with MeV Ultrafast Electron Diffraction. *Proceedings of the National Academy of Sciences* **2022**, *119* (4), e2111949119. https://doi.org/10.1073/pnas.2111949119.

(39) Lindsey, R. K.; Fried, L. E.; Goldman, N. ChIMES: A Force Matched Potential with Explicit Three-Body Interactions for Molten Carbon. *J. Chem. Theory Comput.* **2017**, *13* (12), 6222–6229. https://doi.org/10.1021/acs.jctc.7b00867.

(40) Thompson, A. P.; Aktulga, H. M.; Berger, R.; Bolintineanu, D. S.; Brown, W. M.; Crozier, P. S.; in 't Veld, P. J.; Kohlmeyer, A.; Moore, S. G.; Nguyen, T. D.; et al. LAMMPS - a Flexible Simulation Tool for Particle-Based Materials Modeling at the Atomic, Meso, and Continuum Scales. *Computer Physics Communications* **2022**, *271*, 108171. https://doi.org/10.1016/j.cpc.2021.108171.

(41) Lindsey, R.; Bastea, S.; Hamel, S.; Lyu, Y.; Goldman, N.; Lordi, V. ChIMES Carbon 2.0: A Transferable Machine-Learned Interatomic Model Harnessing Multifidelity Training Data. *ChemRxiv* **2024**. https://doi.org/10.26434/chemrxiv-2024-s1fs5-v2.

(42) Kresse, G.; Furthmüller, J. Efficiency of Ab-Initio Total Energy Calculations for Metals and Semiconductors Using a Plane-Wave Basis Set. *Computational Materials Science* **1996**, *6* (1), 15–50. https://doi.org/10.1016/0927-0256(96)00008-0.

(43) Kresse, G.; Furthmüller, J. Efficient Iterative Schemes for Ab Initio Total-Energy Calculations Using a Plane-Wave Basis Set. *Phys. Rev. B* **1996**, *54* (16), 11169–11186. https://doi.org/10.1103/PhysRevB.54.11169.
(44) Kresse, G.; Hafner, J. Ab Initio Molecular Dynamics for Liquid Metals. *Phys. Rev. B* **1993**, *47* (1), 558–561. https://doi.org/10.1103/PhysRevB.47.558.
(45) Kresse, G.; Hafner, J. Ab Initio Molecular-Dynamics Simulation of the Liquid-Metal--Amorphous-Semiconductor Transition in Germanium. *Phys. Rev. B* **1994**, *49* (20), 14251–14269. https://doi.org/10.1103/PhysRevB.49.14251.
(46) Perdew, J. P.; Burke, K.; Ernzerhof, M. Generalized Gradient Approximation Made Simple. *Phys. Rev. Lett.* **1996**, *77* (18), 3865–3868. https://doi.org/10.1103/PhysRevLett.77.3865.
(47) Perdew, J. P.; Burke, K.; Ernzerhof, M. Generalized Gradient Approximation Made Simple [Phys. Rev. Lett. 77, 3865 (1996)]. *Phys. Rev. Lett.* **1997**, *78* (7), 1396–1396. https://doi.org/10.1103/PhysRevLett.78.1396.
(48) Kononenko, V. V.; Kononenko, T. V.; Pimenov, S. M.; Sinyavskii, M. N.; Konov, V. I.; Dausinger, F. Effect of the Pulse Duration on Graphitisation of Diamond during Laser Ablation. *Quantum Electron.* **2005**, *35* (3), 252. https://doi.org/10.1070/QE2005v035n03ABEH002900.
(49) Heimann, P.; Hartley, N. J.; Inoue, I.; Tkachenko, V.; Antoine, A.; Dorchies, F.; Falcone, R.; Gaudin, J.; Höppner, H.; Inubushi, Y.; et al. Non-Thermal Structural Transformation of Diamond Driven by x-Rays. *Structural Dynamics* **2023**, *10* (5), 054502. https://doi.org/10.1063/4.0000193.
(50) Ogawa, Y.; Ota, M.; Nakamoto, K.; Fukaya, T.; Russell, M.; Zohdi, T. I.; Yamazaki, K.; Aoyama, H. A Study on Machining of Binder-Less Polycrystalline Diamond by Femtosecond Pulsed Laser for Fabrication of Micro Milling Tools. *CIRP Annals* **2016**, *65* (1), 245–248. https://doi.org/10.1016/j.cirp.2016.04.081.
(51) Brown, C. R. D.; Gericke, D. O.; Cammarata, M.; Cho, B. I.; Döppner, T.; Engelhorn, K.; Förster, E.; Fortmann, C.; Fritz, D.; Galtier, E.; et al. Evidence for a Glassy State in Strongly Driven Carbon. *Sci Rep* **2014**, *4* (1), 5214. https://doi.org/10.1038/srep05214.
(52) Riffe, E. J.; Bernal, F.; Kamal, C.; Mizuno, H.; Lindsey, R. K.; Hamel, S.; Raj, S. L.; Hull, C. J.; Kwon, S.; Park, S. H.; et al. Time-Resolved X-Ray Emission Spectroscopy and Resonant Inelastic X-Ray Scattering Spectroscopy of Laser Irradiated Carbon. *J. Phys. Chem. B* **2024**, *128* (26), 6422–6433. https://doi.org/10.1021/acs.jpcb.4c02862.
(53) Lee, R. W.; Moon, S. J.; Chung, H.-K.; Rozmus, W.; Baldis, H. A.; Gregori, G.; Cauble, R. C.; Landen, O. L.; Wark, J. S.; Ng, A.; et al. Finite Temperature Dense Matter Studies on Next-Generation Light Sources. *J. Opt. Soc. Am. B, JOSAB* **2003**, *20* (4), 770–778. https://doi.org/10.1364/JOSAB.20.000770.

TOC GRAPHICS